Cell Metabolism
Article

A Central Thermogenic-like Mechanism in Feeding Regulation: An Interplay between Arcuate Nucleus T3 and UCP2

Anna Coppola,[1] Zhong-Wu Liu,[1,4] Zane B. Andrews,[1] Eric Paradis,[5] Marie-Claude Roy,[5] Jeffrey M. Friedman,[6] Daniel Ricquier,[7] Denis Richard,[5] Tamas L. Horvath,[1,2,3] Xiao-Bing Gao,[1] and Sabrina Diano[1,2,*]
[1] Department of Obstetrics, Gynecology & Reproductive Sciences
[2] Department of Neurobiology
[3] Section of Comparative Medicine
Yale University School of Medicine, New Haven, CT 06520, USA
[4] Department of Neurobiology, Yunyang Medical College, Shiyan, Hubei, 442000, China
[5] Brown Research Chair on Obesity, Laval Hospital Research Center, Université Laval, Quebec, QC G1V 4G5, Canada
[6] Laboratory of Molecular Genetics, Rockefeller University, New York, NY 10021, USA
[7] CNRS Unit 9078, Université René Descartes, Faculté de Médecine, Site Necker, 156 Rue de Vaugirard, 75015 Paris, France
*Correspondence: sabrina.diano@yale.edu
DOI 10.1016/j.cmet.2006.12.002

SUMMARY

The active thyroid hormone, triiodothyronine (T3), regulates mitochondrial uncoupling protein activity and related thermogenesis in peripheral tissues. Type 2 deiodinase (DII), an enzyme that catalyzes active thyroid hormone production, and mitochondrial uncoupling protein 2 (UCP2) are also present in the hypothalamic arcuate nucleus, where their interaction and physiological significance have not been explored. Here, we report that DII-producing glial cells are in direct apposition to neurons coexpressing neuropeptide Y (NPY), agouti-related protein (AgRP), and UCP2. Fasting increased DII activity and local thyroid hormone production in the arcuate nucleus in parallel with increased GDP-regulated UCP2-dependent mitochondrial uncoupling. Fasting-induced T3-mediated UCP2 activation resulted in mitochondrial proliferation in NPY/AgRP neurons, an event that was critical for increased excitability of these orexigenic neurons and consequent rebound feeding following food deprivation. These results reveal a physiological role for a thyroid-hormone-regulated mitochondrial uncoupling in hypothalamic neuronal networks.

INTRODUCTION

Thyroid hormones play major roles during development as well as in adulthood. In adults, an important contribution of the thyroid gland is to regulate metabolism at both the cellular and whole-organism levels. Various downstream transcriptional events triggered by the active thyroid hormone, triiodothyronine (T3), have been thought to alter cell and tissue metabolism (see Bassett et al., 2003 for review). In addition, nontranscriptional effects of T3 have also been identified (see Bassett et al., 2003; Harvey and Williams, 2002; Weitzel et al., 2003 for review). With regard to whole-animal physiology, a key role for T3 was established in the regulation of brown-fat-associated nonshivering thermogenesis (see Silva, 1995 for review). The molecular underpinning of thermogenesis in brown fat is the activation of mitochondrial uncoupling protein 1 (UCP1), which dissipates energy in the form of heat (see Ricquier, 2005; Nedergaard et al., 2005 for review). UCP1 activation is associated with increased proton conductance of the inner mitochondrial membrane and mitochondrial proliferation (Ricquier, 2005; Nedergaard et al., 2005). The activation of UCP1 is under the control of the sympathetic nervous system and fatty acids (Sell et al., 2004), and it is regulated by T3 (Reitman et al., 1999; Lanni et al., 2003). Based on structure homology, other UCPs with varying tissue distribution were also discovered, including UCP2 and UCP3, but their physiological role remains ill defined and tissue specific (Krauss et al., 2005). In contrast to UCP1, UCP2 and UCP3 are conditional uncouplers yielding less robust changes in proton permeability of the inner mitochondrial membrane (see Andrews et al., 2005a; Brand and Esteves, 2005 for review), and their function is not dependent on sympathetic activation but can be altered by T3 (Horrum et al., 1990; Kalderon et al., 1995). The hypothalamic arcuate nucleus, which is considered to be the key brain site that responds to changes in peripheral tissue metabolism (see Schwartz et al., 2000 for review), expresses high levels of UCP2 (Horvath et al., 1999) as well as thyroid hormone receptors (Lechan et al., 1993) and also has the capacity for local production of T3 (Coppola et al., 2005a, 2005b). To date, however, it is unclear whether local thyroid hormone production affects arcuate nucleus UCP activity and, if so, whether such an interaction has any physiological relevance in the regulation of energy metabolism.

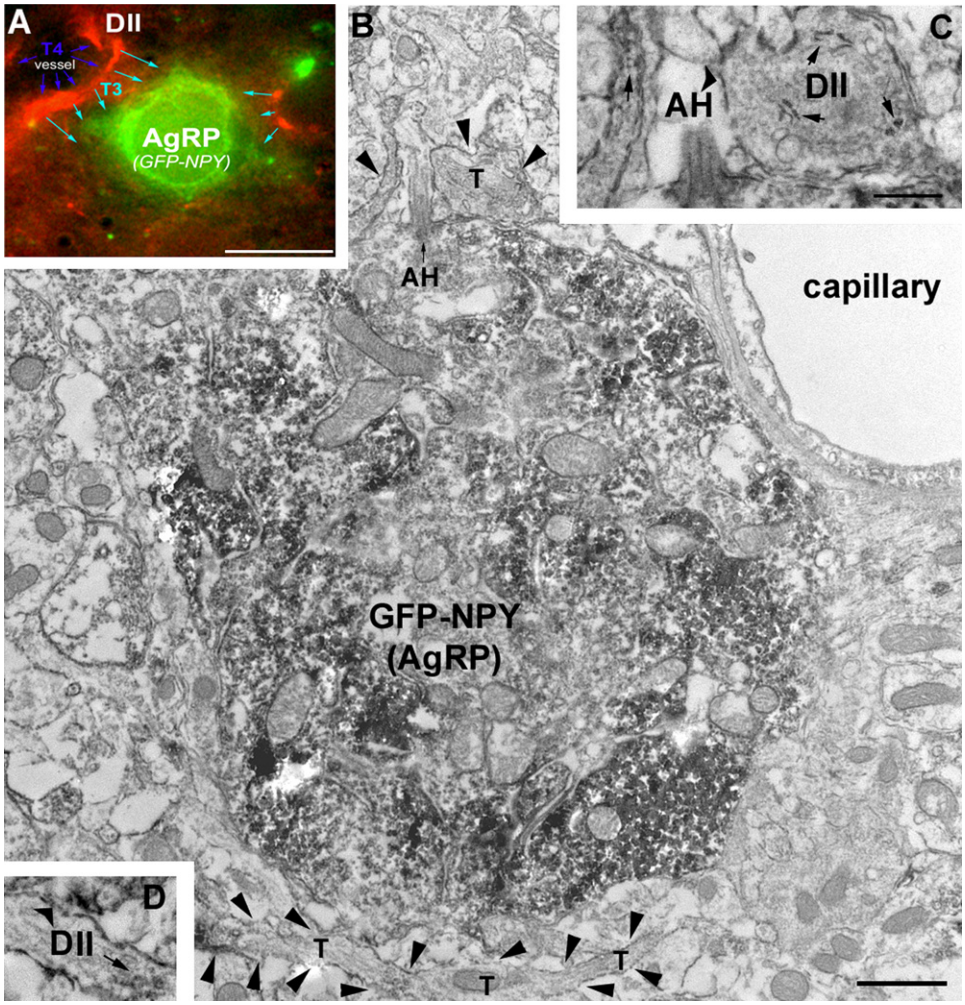

Figure 1. DII-Producing Glia Are Associated with Orexigenic Neurons

(A) Immunostaining for DII (red fluorescence) in GFP-NPY transgenic mice reveals a close association between DII-producing glial processes and NPY/AgRP neurons (green fluorescence). Scale bar = 10 μm.

(B) Electron micrograph of tanycytes immunostained with DII (arrowheads) in contact with a GFP-NPY immunoreactive cell. Scale bar = 1 μm.

(C) High-magnification micrograph showing a tanycyte (T) immunopositive for DII (arrows point to immunostaining in the endoplasmic reticulum) in-contact (arrowheads) with an axon hillock (AH) of a GFP-NPY cell in the arcuate nucleus of the hypothalamus. Scale bar in (C) (also valid for [D]) = 500 nm.

(D) Another tanycyte immunostained for DII (arrow points to the immunoreactivity of the endoplasmic reticulum) in contact (arrowhead) with the same GFP-NPY cell of the arcuate nucleus.

RESULTS

DII-Producing Glia Are Associated with Orexigenic Neurons

Local T3 production is catalyzed by type II deiodinase (DII) expressed in arcuate nucleus glial cells (Tu et al., 1997; Diano et al., 1998a, 1998b, 2003a), and both DII activity and local T3 production are increased during fasting (Coppola et al., 2005a, 2005b). UCP2, on the other hand, is expressed exclusively in neurons of the arcuate nucleus (Horvath et al., 1999), including cells that produce neuropeptide Y (NPY) and agouti-related protein (AgRP) (Horvath et al., 1999). These orexigenic cells of the brain are mandatory for feeding regulation (Gropp et al., 2005; Luquet et al., 2005), and their electrical activity is enhanced during fasting (Takahashi and Cone, 2005) when local T3 production is increased (Coppola et al., 2005b). Thus, we first analyzed whether a relationship exists between arcuate nucleus DII-expressing glial cells and NPY/AgRP neurons. Immunostaining for DII in GFP-NPY transgenic mice revealed a close association between DII-producing glial processes (red fluorescence) and NPY/AgRP neurons (green fluorescence; Figure 1A). Electron microscopic examination confirmed that DII-immunopositive tanycytes (arrows pointing to the immunoreactivity of the endoplasmic reticulum, Figures 1B–1D) made contact with

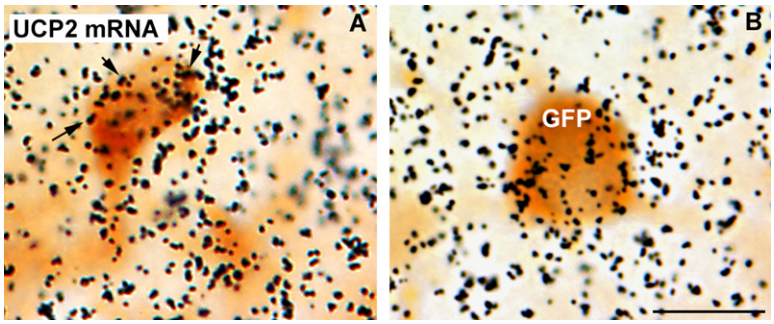

Figure 2. UCP2 in NPY/AgRP Neurons
Representative light micrographs showing the results of combined in situ hybridization for UCP2 (silver grain representing *UCP2* mRNA) and immunocytochemistry for GFP in GFP-NPY mice (light brown diaminobenzidine reaction product). Scale bar = 10 μm.

GFP-NPY immunoreactive cells (arrowheads). Thus, it would appear possible that the orexigenic NPY/AgRP neurons are exposed to locally formed T3.

UCP2 in NPY/AgRP Neurons

We previously showed that UCP2 immunoreactivity is expressed in the arcuate NPY neurons (Horvath et al., 1999). To confirm that *UCP2* mRNA is present in these same cells, in situ hybridization for UCP2 was performed in GFP-NPY mice. *UCP2* mRNA was expressed in various brain regions as previously reported (Richard et al., 1998; Horvath et al., 1999). Intense labeling was found in the hypothalamus, where several nuclei showed a strong hybridization signal including the preoptic area, as well as the suprachiasmatic, paraventricular, and ventromedial nuclei. The intensity of the signal was markedly greater in the arcuate nucleus. When combined with immunocytochemistry for GFP-NPY, we found that GFP-NPY-labeled neurons (light brown diaminobenzidine reaction) coexpressed *UCP2* mRNA (silver grain representing *UCP2* mRNA, Figure 2).

Hypothalamic DII-Associated T3 Levels Are Elevated during Fasting

We have shown that during food deprivation, *DII* mRNA and activity levels are increased in the hypothalamus (Diano et al., 1998a; Coppola et al., 2005a). Moreover, we recently demonstrated that the elevation in DII activity also induces increased tissue levels of T3 in rats (Coppola et al., 2005b). To confirm that this also occurs in mice, we performed T3 measurements in the hypothalamic tissues of fasted and fed mice. As reported earlier (Coppola et al., 2005b), hypothalamic T3 levels were significantly higher in fasted mice (4.77 ± 1.045 pg/mg wet tissue) compared to ad libitum-fed animals (2.29 ± 0.21 pg/mg wet tissue; Figure 3A).

Fasting or T3 Administration Induces Hypothalamic Uncoupling Activity

We analyzed whether uncoupling activity of the arcuate nucleus is induced by fasting or T3 administration by measuring the uncoupling activity in isolated hypothalamic mitochondria of fasted, fed, T3-treated, and saline-treated animals. Serum free T3 levels in T3-treated mice were significantly higher (27.14 ± 2.5 pg/ml) than the saline controls (1.24 ± 0.09 pg/ml). The ratio of hypothalamic FFA-induced uncoupling to state 4 respiration (baseline uncoupling) was significantly elevated in T3-treated (6.9 ± 0.28 versus 4.3 ± 0.14 of saline-treated animals) and fasted wild-type animals (5.96 ± 0.16 versus 4.16 ± 0.19 of fed animals) (Figure 3B).

Increased Hypothalamic Mitochondrial Uncoupling Activity during Fasting Is UCP2 Dependent and Nucleotide Regulated

To analyze whether the increase in hypothalamic mitochondrial uncoupling activity was UCP2 dependent and GDP regulated, we analyzed the effect of fasting or T3 administration on hypothalamic uncoupling activity in *UCP2* KO animals. Neither of these interventions altered mitochondrial uncoupling in *UCP2* KO animals (Figure 3B). To test whether changes in expression levels of the adenine nucleotide translocator (ANT), a mitochondrial protein that is regulated by thyroid hormones in the periphery (Dummler et al., 1996) and was shown to alter mitochondrial uncoupling (Brustovetsky et al., 1990; Skulachev, 1991, 1998; Brustovetsky and Klingenberg, 1994), may also be associated with increased hypothalamic uncoupling, we measured *ANT* mRNA levels by real-time PCR after fasting or T3 treatment. Fasting did not alter *ANT* mRNA levels (0.83 ± 0.03) compared to fed controls (0.79 ± 0.06). On the other hand, T3 treatment induced a slight but significant elevation of *ANT* mRNA levels (0.92 ± 0.03) compared to saline controls (0.82 ± 0.03). However, because T3 administration did not induce elevated fatty-acid-driven mitochondrial uncoupling in *UCP2* KO mice, it is reasonable to suggest that the role of ANT in fasting-induced hypothalamic mitochondrial uncoupling is negligible.

To analyze whether UCP2-dependent mitochondrial uncoupling during fasting is nucleotide regulated, we measured uncoupling activity in either the presence or absence of GDP. When GDP was added to the respiration buffer, the fasting-induced increase in the ratio of palmitate-induced uncoupling to baseline uncoupling (5.96 ± 0.16 versus 4.16 ± 0.19 of fed animals) was abolished (GDP-treated fasted, 4.14 ± 0.31; GDP-treated fed, 4.31 ± 0.002; p = 0.64).

T3 Regulates Hypothalamic UCP2 Expression

To test whether a relationship exists between hypothalamic T3 levels and UCP2 transcription, we measured

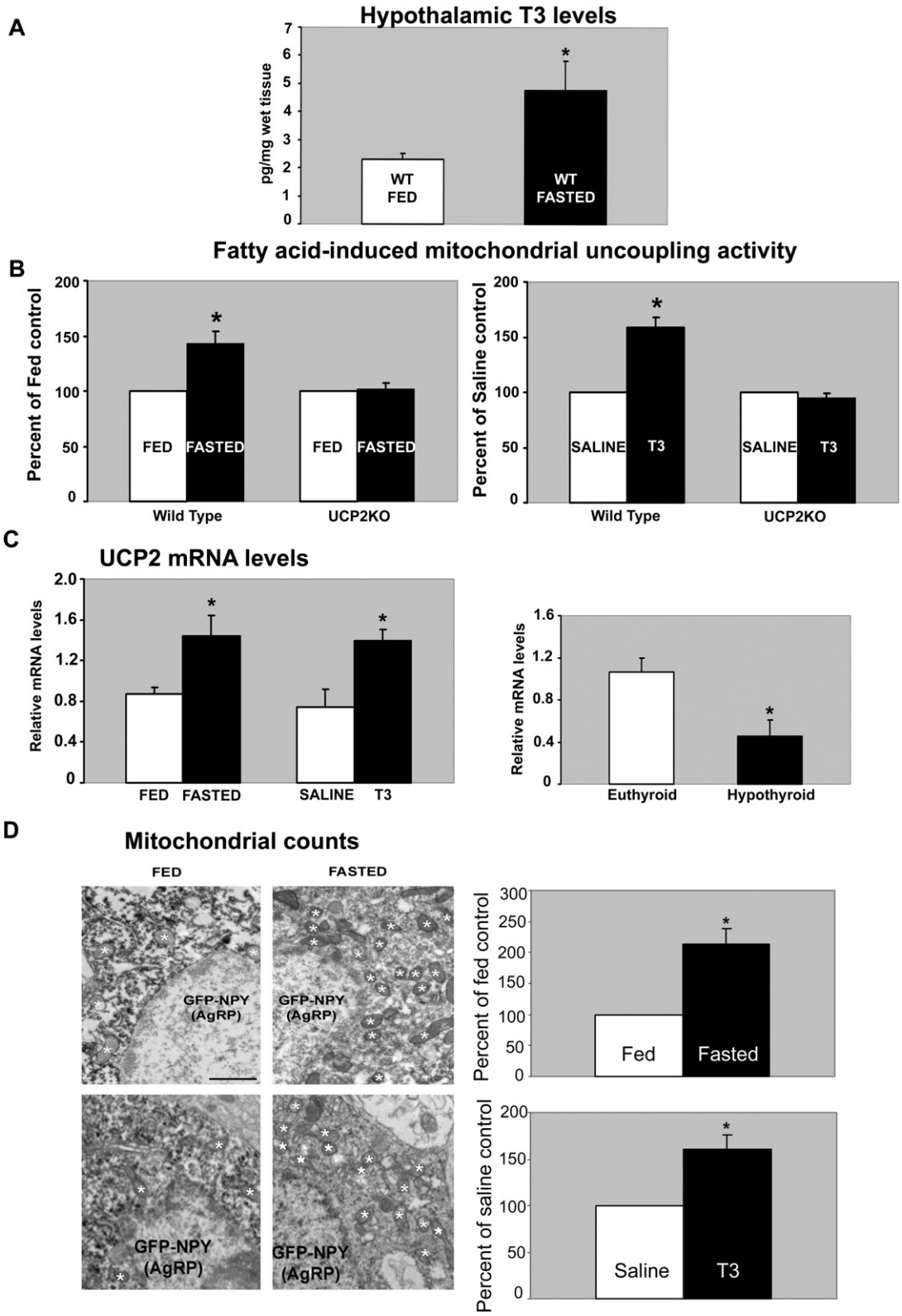

Figure 3. Fasting and T3 Induce Hypothalamic *UCP2* Activity and mRNA Levels and an Increase in Mitochondrial Density

(A) Graph showing hypothalamic T3 levels in fed and 24 hr fasted wild-type (WT) animals. Values are expressed as mean ± SEM.

(B) Fatty-acid-induced uncoupling in fasted, fed, T3-treated, and saline-treated mice. Exposure to the free fatty acid palmitate induces increased mitochondrial uncoupling in fasted mice compared to their fed controls (left) and T3-treated mice compared to saline-treated mice (right). The

UCP2 mRNA levels in the hypothalamus of fasted, T3-treated, and propylthiouracil (PTU) + iopanoic acid (IOP)-treated mice. Fasting (1.44 ± 0.2 versus 0.9 ± 0.07 of fed mice) and T3 treatment (1.40 ± 0.11 versus 0.7 ± 0.2 of saline-treated mice) induced a significant increase in hypothalamic *UCP2* mRNA levels (Figure 3C). Under hypothyroid conditions, in which the production of thyroid hormones as well as the activity of all the deiodinases was inhibited (by PTU or PTU+IOP, respectively), hypothalamic *UCP2* mRNA levels were significantly lower (0.45 ± 0.15) than those of euthyroid control mice (1.06 ± 0.1; Figure 3C).

Increased Mitochondrial Uncoupling Is Associated with Elevated Mitochondrial Density in NPY/AgRP Neurons

Increased mitochondrial uncoupling induces mitochondrial proliferation in both brown fat (see Klingenspor, 2003 for review) and brain (Diano et al., 2003b). Thus, we tested whether increased mitochondrial density is also associated with increased UCP2 activity in the arcuate nucleus during fasting or T3 administration by stereological assessment of mitochondrial number in NPY/AgRP neurons of fasted and fed GFP-NPY mice and saline- and T3-treated mice. In NPY/AgRP neurons, fasting induced an approximately 200% rise in mitochondrial number (Figure 3D). Similarly, in the NPY/AgRP neurons of T3-treated mice, the number of mitochondria was 160% higher than in those of their saline-treated controls (Figure 3D).

Lack of UCP2 Blunts NPY/AgRP Neuronal Responses to Fasting

c-Fos Activation

To analyze whether the lack of UCP2 could affect the activation of arcuate neurons, we first examined c-*fos* mRNA in the arcuate nucleus of *UCP2* KO mice and wild-type controls after 24 hr fasting. We found that c-*fos* mRNA induction by fasting was blunted in *UCP2* KO animals compared to wild-type littermates (Figure 4A). In accordance with the mRNA study, immunocytochemistry for c-Fos in the arcuate nucleus showed that *UCP2* KO mice exhibited just 41% of c-Fos staining compared to their wild-type controls (Figure 4B). Next we performed double immunocytochemistry for GFP-NPY and c-Fos and observed that in wild-types, 71% of the GFP-NPY cells were c-Fos positive, whereas in *UCP2* KO mice, only 27% of this cell population expressed c-Fos (Figure 4B). It is noteworthy that no difference in the number of NPY neurons in the wild-type controls and *UCP2* KO animals was found (data not shown).

NPY *and* POMC *Gene Expression in Fed and Fasted Wild-Type and* UCP2 *KO Mice*

To assess whether the lack of UCP2 would impair the induction of *NPY* mRNA during fasting, we performed real-time PCR on hypothalamic tissues from wild-type and *UCP2* KO mice in fed and fasted conditions. In wild-type animals, fasting significantly increased *NPY* mRNA levels (2.51 ± 0.17; Figure 4C) compared to animals fed ad libitum (1.03 ± 0.26; Figure 4C). On the other hand, in *UCP2* KO mice, fasting did not induce the increase in *NPY* mRNA (1.24 ± 0.3; Figure 4C) seen in wild-type mice (1.18 ± 0.16; Figure 4C). Note, however, that no difference in *NPY* mRNA levels was found in fed wild-type and *UCP2* KO animals.

We then analyzed *POMC* mRNA and found that, in contrast to *NPY*, *POMC* mRNA levels in *UCP2* KO animals showed the same changes as the wild-type controls. In wild-type mice, fasting induced a decrease in *POMC* mRNA (0.62 ± 0.12) compared to fed controls (1.004 ± 0.05). Similarly, fasted *UCP2* KO animals showed a significant reduction of *POMC* mRNA (0.66 ± 0.03) compared to fed *UCP2* KO mice (1.011 ± 0.06).

Mitochondrial Density

Coinciding with the lack of UCP2 activation by fasting, the mitochondrial density within the NPY neurons did not change after a 24 hr fast in *UCP2* KO animals (0.19 ± 0.02 per μm^2 in fed *UCP2* KO; 0.16 ± 0.02 per μm^2 in fasted *UCP2* KO; $p = 0.2$). When we compared the mitochondrial number of fasted *UCP2* KOs with their fasted wild-type littermates, *UCP2* KO mice exhibited only 30% of the number of mitochondria seen in the wild-type controls (Figure 5A).

Electrophysiology

To determine whether the electrical activity of NPY neurons is also affected in *UCP2* KO mice during fasting, we analyzed the firing rate of GFP-NPY neurons. In order to keep intracellular content intact to eliminate the run-down of action potentials during the entire experiment, extracellular recording of spikes was performed in fasted wild-type and fasted *UCP2* KO mice. We found that during fasting in both wild-type and *UCP2* KO mice, the firing rate of the arcuate NPY neurons was highly heterogeneous. After fasting, the firing rate was 44 to 717 spikes per minute (median frequency = 157 per minute; n = 16) in wild-type mice and 0 to 1029 spikes per minute (median

increase in uncoupling activity is due specifically to the elevation in UCP2 since *UCP2* KO mice showed no alteration in uncoupling activity following either fasting (left panel) or T3 treatment (right panel). Data are expressed as the percentage of increase above oligomycin-induced state 4 respiration (±SEM).

(C) Increase in hypothalamic *UCP2* mRNA in fasted compared to fed controls and T3-treated compared to saline-treated mice (left). On the other hand, *UCP2* mRNA was downregulated under hypothyroid conditions (right). The graphs show the expression levels of *UCP2* mRNA (±SEM) relative to the expression levels in fed or saline-treated mice.

(D) Representative electron micrographs of GFP-NPY neurons in the hypothalamic arcuate nucleus of a fed and fasted mouse (upper micrographs) and a T3-treated and saline-treated mouse (lower micrographs). White asterisks indicate some of the mitochondria that appear to be more numerous in fasted and T3-treated NPY/AgRP neurons compared to their respective controls. Scale bar = 1 μm. Unbiased stereological and statistical analyses confirmed that the mitochondrial number in NPY/AgRP neurons (±SEM) in fasted and T3-treated arcuate nuclei was significantly higher compared to the values of their respective controls. *$p < 0.05$ compared to fed animals, saline-treated mice, or hypothyroid controls.

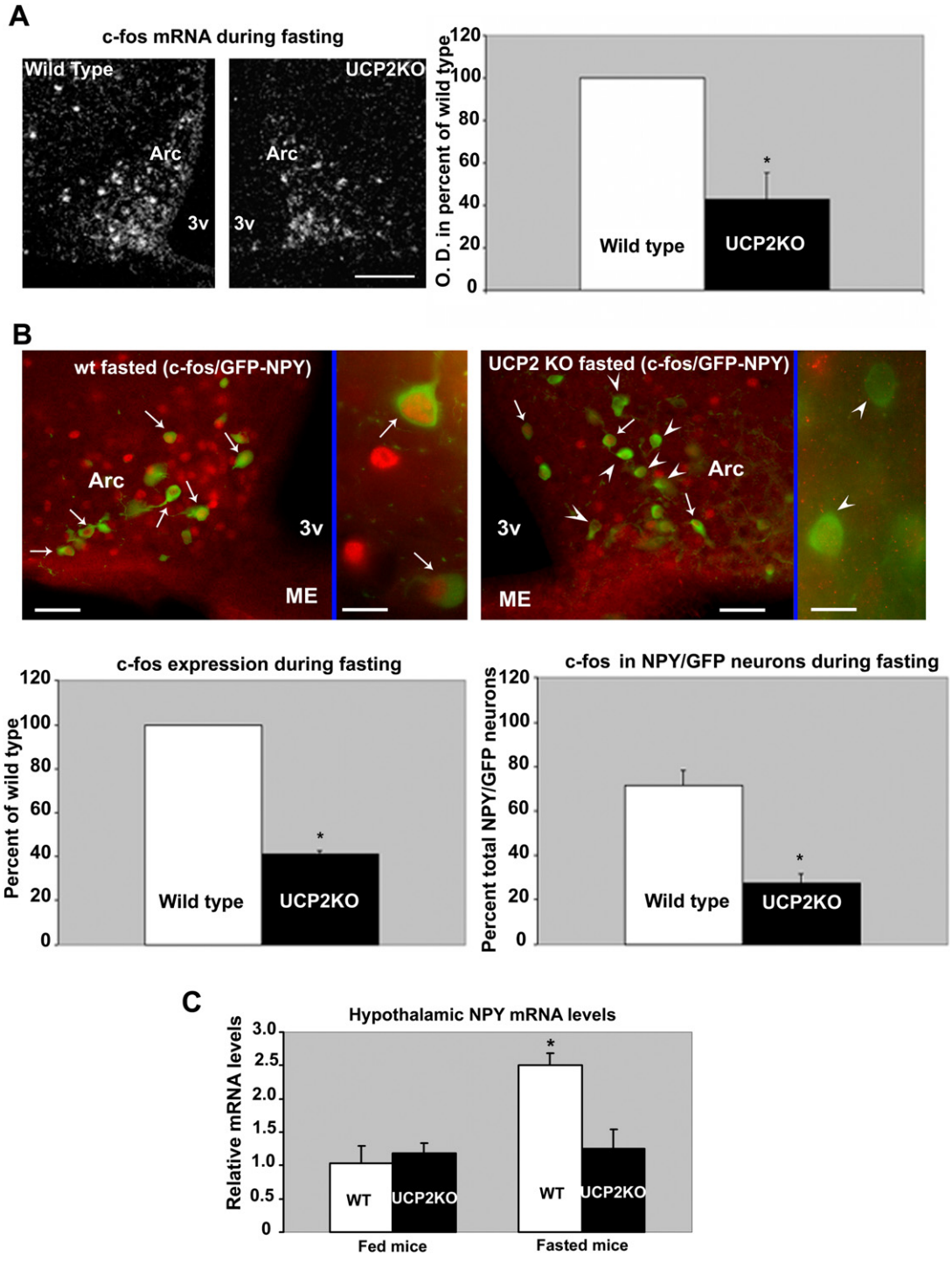

Figure 4. Lack of UCP2 Decreases c-Fos Expression in NPY/AgRP Neurons and Prevents the Elevation of *NPY* mRNA Levels during Fasting

(A) Representative black-field micrographs of c-*fos* mRNA expression in the arcuate nucleus of wild-type and *UCP2* KO mice following 24 hr of fasting. Arc = arcuate nucleus; 3v = third ventricle; scale bar = 100 μm. The graph shows the significant decrease in c-*fos* mRNA (±SEM) in *UCP2* KO mice compared to their wild-type controls. *$p < 0.05$.

(B) Low- and high-power magnification of c-Fos and GFP staining in the arcuate nucleus of GFP-NPY mice (WT) and *UCP2* KO/GFP-NPY mice (*UCP2* KO) following 24 hr of fasting. Note the difference in the amount of c-Fos staining in the wild-type compared to the *UCP2* KO mouse. Arrows show cells double labeled for GFP and c-Fos, while arrowheads indicate GFP immunopositive neurons that are negative for c-Fos staining. Graphs show the percentage of c-Fos-immunopositive nuclei (±SEM) in the arcuate nucleus of *UCP2* KO mice compared to that of wild-type controls and the percentage of cells double stained for c-Fos and GFP in GFP-NPY mice and *UCP2* KO-GFP-NPY mice compared to the total number of GFP-NPY neurons

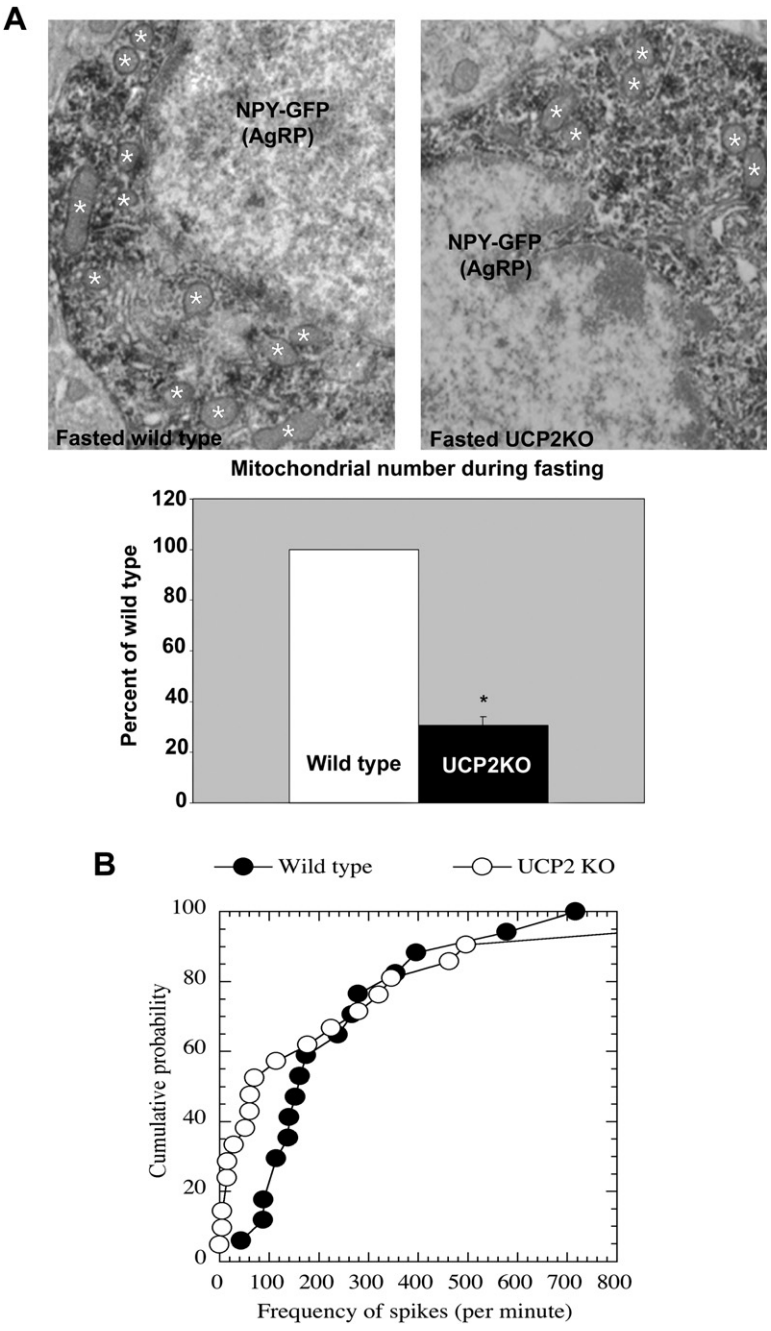

Figure 5. Lack of UCP2 Prevents Fasting-Induced Increase in Mitochondrial Density and Alters Electrical Properties

(A) Representative electron micrographs of GFP-NPY neurons in the hypothalamic arcuate nucleus of 24 hr-fasted wild-type and *UCP2* KO mice. White asterisks indicate some of the mitochondria that appear to be less numerous in fasted *UCP2* KO NPY/AgRP neurons compared to the controls. Scale bar = 1 μm. Unbiased stereological and statistical analyses confirmed this observation. *$p < 0.05$ compared to wild-type mice.

(B) Cumulative probability curves for frequency of spikes recorded from arcuate GFP-NPY neurons of fasted wild-type and fasted *UCP2* KO mice show that the frequency of spike firing is significantly lower in *UCP2* KO mice than in wild-type controls. The median frequency of spikes of GFP-NPY neurons was 157 per minute for wild-type and 71 per minute for *UCP2* KO mice. The distributions of the frequency of spikes from these two groups are significantly different as indicated by the Kolmogorov-Smirnov test ($p < 0.05$).

frequency = 71 per minute; n = 21) in *UCP2* KO mice. Thus, we generated cumulative probability curves for frequencies of spikes recorded from wild-type and *UCP2* KO mice, as shown in Figure 5B. The cumulative probability curve for *UCP2* KO mice shifted to the left compared to that of wild-type mice. The distribution of the frequencies of spikes from these two groups was significantly different as indicated by the Kolmogorov-Smirnov test ($p < 0.05$). In summary, our data show that the frequency of spike firing is significantly lower in *UCP2* KO mice than in wild-types after fasting, which is reflected by relatively more NPY neurons firing at a low frequency.

within the arcuate nucleus. It is noteworthy that no difference in the number of NPY neurons was found between wild-type controls and *UCP2* KO animals (data not shown). Scale bars in low- and high-magnification micrographs represent 50 μm and 10 μm, respectively. 3v = third ventricle; Arc = arcuate nucleus; ME = median eminence. *$p < 0.001$ compared to wild-type controls.

(C) Expression levels of *NPY* mRNA relative to expression levels in fed wild-type and fed *UCP2* KO mice (±SEM). Following fasting, wild-type animals exhibited an increase in *NPY* mRNA levels, while fasted *UCP2* KO mice did not show this elevation.

Diminished Rebound Feeding in Animals Lacking Either UCP2 or DII

It has been shown that NPY/AgRP neurons are critical for feeding (Gropp et al., 2005; Luquet et al., 2005). Thus, to test whether UCP2-dependent cellular mechanisms in NPY neurons are important for appropriate feeding responses, we analyzed the rebound feeding of *UCP2* KO and wild-type animals after 24 hr fasting. The initial feeding response of *UCP2* KO animals to a 24 hr fast was diminished (0.52 ± 0.13 g; 0.35 ± 0.03 g after the first hour of food) compared to the values of fasted wild-type littermates (0.86 ± 0.09 g; 0.54 ± 0.05 g after the second hour of food; Figure 6A). Note, however, that the normal feeding behavior of these animals is not affected, nor do they show visible signs of gross metabolic alterations (Arsenijevic et al., 2000; Zhang et al., 2001). These observations indicate that UCP2 may be necessary for activation of the arcuate nucleus orexigenic NPY/AgRP neurons to evoke an appropriate response to fasting.

Because we showed that DII-produced T3 plays a role in UCP2 activation during fasting, we analyzed the acute responses of *DII* knockout animals (DIIKO; Schneider et al., 2001) to a 24 hr fasting regimen. Fifteen male DIIKO and six male wild-type animals were fasted. Six hours before food was replaced, seven DIIKO mice were injected intraperitoneally (i.p.) with T3. Food was replaced after 24 hr, at which time body weight and core body temperature were recorded, and food intake was measured in a 30 min period following refeeding. Food intake at the end of the 24 hr fast was significantly lower in DIIKO animals compared to wild-type littermates in the first 30 min after refeeding (0.38 ± 0.05 g in DIIKO; 0.65 ± 0.02 in the wild-type; Figure 6B). When DIIKO mice were treated with T3, food intake was significantly increased compared to saline-treated DIIKO mice (0.57 ± 0.05) in both the first and second 30 min periods after refeeding (0.39 ± 0.05 g in T3-treated DIIKO; 0.18 ± 0.05 g in saline-treated DIIKO; 0.24 ± 0.02 g in the wild-type after the second hour of food; Figure 6B).

Lack of DII Prevents the Increase in Hypothalamic *T3* and *NPY* mRNA Levels during Fasting

Finally, we analyzed whether the reduction in food intake after fasting seen in DIIKO mice was associated with hypothalamic *T3* and *NPY* mRNA levels. First, the serum levels of free T4 and free T3 in wild-type and DIIKO animals were analyzed. As previously reported, fasting decreased serum T4 and T3 levels (3.3 ± 0.06 ng/dl and 0.35 ± 0.021 pg/ml, respectively) compared to ad libitum-fed conditions (6.8 ± 1.1 ng/dl for T4 and 0.51 ± 0.020 pg/ml for T3). Similarly, fasted DIIKO animals showed a significant reduction in serum T4 and T3 levels (4.9 ± 0.6 ng/dl and 0.33 ± 0.023 pg/ml, respectively) compared to fed DIIKO mice (12.6 ± 1.2 ng/dl for T4 and 0.46 ± 0.026 pg/ml for T3). When we examined hypothalamic T3 levels in fasted DIIKO mice, no changes were observed compared to fed DIIKO animals (2.39 ± 0.30 pg/mg wet tissue versus 2.11 ± 0.50 pg/mg wet tissue, respectively; Figure 6C). Note that no difference in hypothalamic T3 levels was observed between fed wild-type and fed DIIKO mice. In addition, supporting the feeding data, hypothalamic *NPY* mRNA levels in fasted DIIKO mice (1.37 ± 0.23; Figure 6C) did not differ compared to the levels of fed DIIKO mice (1.05 ± 0.18; Figure 6C). In contrast to *NPY*, *POMC* mRNA levels in fasted DIIKO mice were significantly decreased (0.72 ± 0.05) compared to fed DIIKO controls (1.004 ± 0.04). This reduction was comparable to that observed in wild-type animals (1.003 ± 0.03 in fed WTs and 0.63 ± 0.09 in fasted WTs).

DISCUSSION

Our results present evidence of a physiological role for UCP2 in hypothalamic neuronal functions. The observed increase in the activity of hypothalamic mitochondrial uncoupling protein 2 is thyroid hormone regulated and nucleotide (GDP) dependent. This T3-regulated mitochondrial uncoupling by UCP2 was found to be critical for the appropriate activation of arcuate nucleus NPY/AgRP neurons during fasting, thereby altering rebound feeding in mice. Because we found that mitochondrial proliferation within NPY/AgRP neurons is inherent to the response to negative energy balance and is UCP2 dependent, we suggest that neuronal UCP2 in the hypothalamus plays an important role in the adaptation of these neurons to changing metabolic demand. These observations provide experimental evidence for the hypothesis that neuronal UCP2 plays a physiological role in the regulation of neuronal functions (Horvath et al., 1999, 2002a, 2002b, 2003; Diano et al., 2003b; Andrews et al., 2005b, 2006).

We first revealed a direct relationship between DII-containing (putative T3-producing) glial elements and the NPY/AgRP-producing arcuate nucleus neurons. We also found that NPY cells express UCP2 and that the expression level and activity of mitochondrial UCP2 are enhanced by fasting or T3 alone but are reduced under hypothyroid conditions. It has been previously demonstrated that T3 increases *UCP2* mRNA and activity in peripheral tissues such as white adipose tissue, skeletal muscle, and heart (Masaki et al., 1997; Lanni et al., 1997). Our results now show that, similar to the periphery, T3 also alters mitochondrial UCP2 activity in the hypothalamus. Mice lacking UCP2 did not exhibit the enhanced uncoupling activity seen following either fasting or T3 treatment. In addition, free-fatty-acid-induced GDP-sensitive uncoupling was prevented in fasted wild-type animals compared to their fed controls, a strong indication that UCP2, rather than other uncouplers, is responsible for the increased uncoupling activity observed in our study.

An increase in mitochondrial number was also observed in the arcuate NPY/AgRP neurons after fasting and T3 treatment, a response that was absent in *UCP2* KO animals. This observation is in line with our earlier demonstration of elevated mitochondrial number in hippocampal pyramidal cells of human UCP2/3-overexpressing mice (Diano et al., 2003b). Whether this change in mitochondrial number relates to fission and fusion of mitochondria or

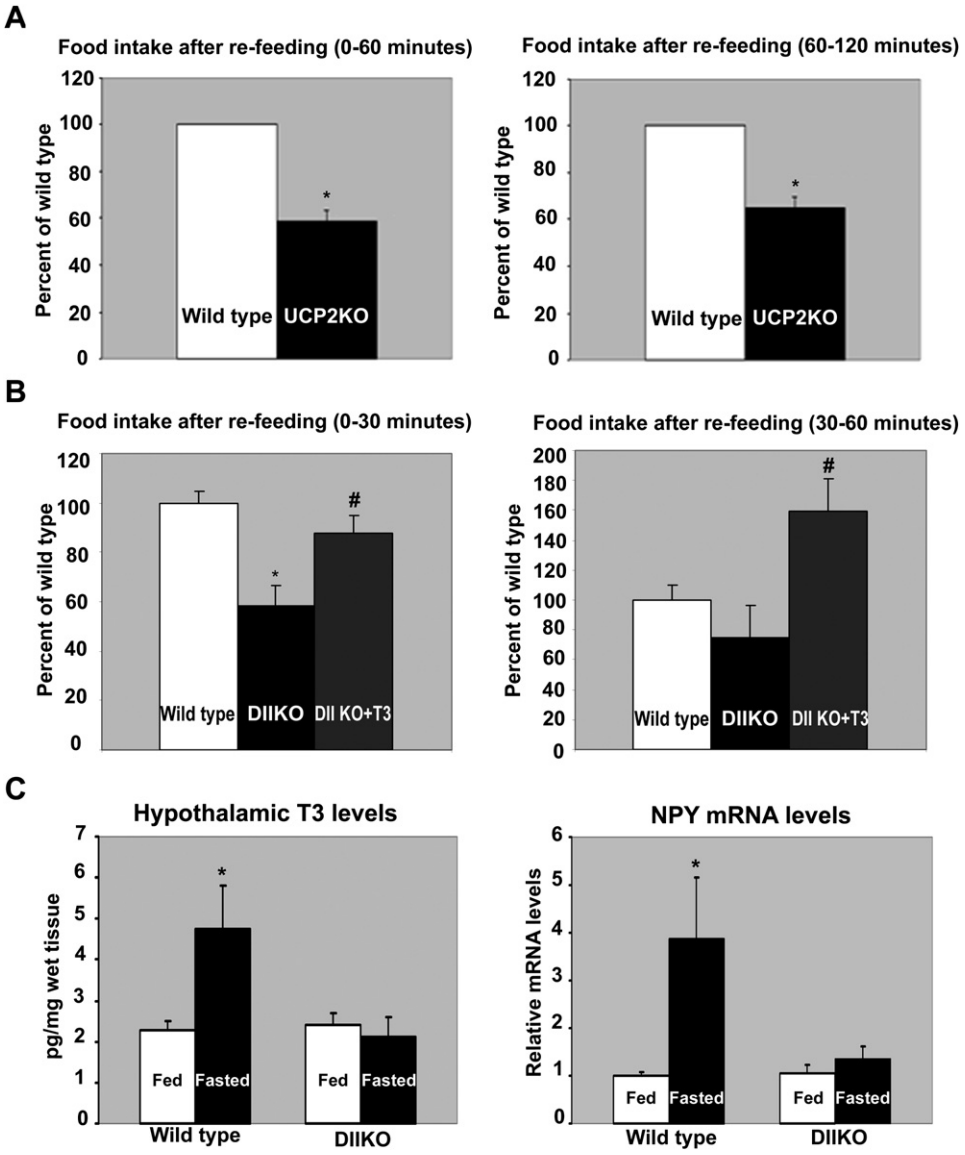

Figure 6. Diminished Rebound Feeding in Animals Lacking Either UCP2 or DII

(A) Percentage of food intake (±SEM) during the first and second hours after 24 hr of fasting in *UCP2* KO mice in relation to wild-type values. *$p < 0.05$ compared to wild-type controls.

(B) Percentage of food intake (±SEM) after 24 hr of fasting in DIIKO mice and DIIKO mice injected with T3 compared to their wild-type controls between 0–30 min and 30–60 min after refeeding. *$p < 0.05$ compared to wild-type controls; #$p < 0.05$ compared to DIIKO.

(C) Hypothalamic T3 levels and *NPY* mRNA levels (±SEM) measured in fed and fasted wild-type and DIIKO mice. *$p < 0.05$ compared to wild-type animals.

whether it also entails de novo mitochondrial biogenesis needs to be further explored. Mitochondrial density increases in neuronal sites with increased energy demand in order to support neurotransmission (Shepherd and Harris 1998; Rowland et al., 2000; Li et al., 2004; Schuman and Chan, 2004). Thus, we suggest that the increase in mitochondrial density in the cell bodies of the NPY neurons is important to provide and maintain the high level of activity of these orexigenic neurons in response to food deprivation. Indeed, such an acute activation of the NPY cells is seen during fasting (Takahashi and Cone, 2005). We propose that although individual mitochondria may be less efficient in producing ATP, overall, due to their increased number, cellular ATP levels may actually rise (Diano et al., 2003b; Andrews et al., 2005b). This, in turn, could play an important role in sustaining the activity of these neurons during negative energy balance. In accordance with this, we observed that, during fasting, c-*fos* mRNA levels in the arcuate nucleus of *UCP2* KO mice were significantly reduced, and arcuate NPY neurons of

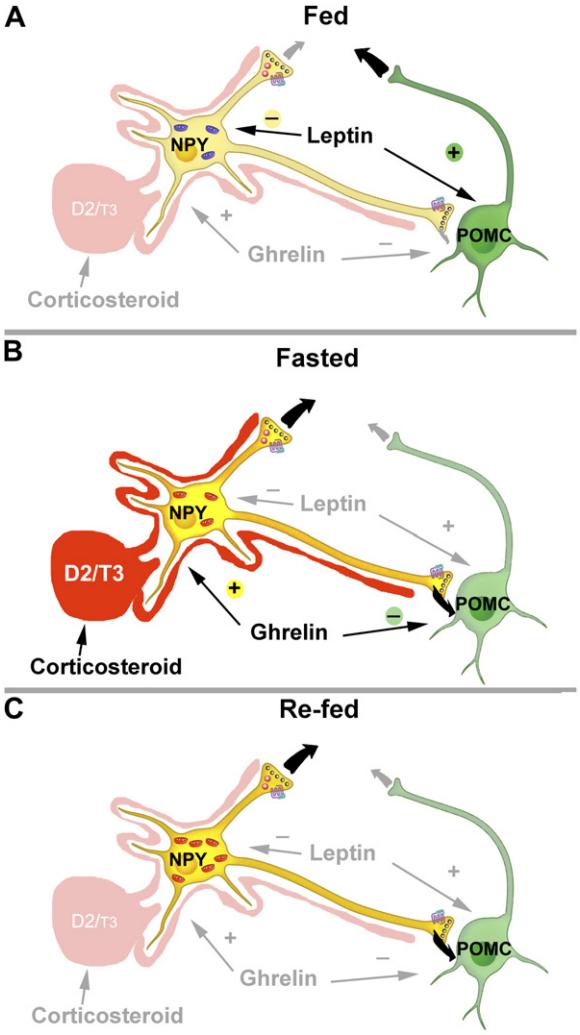

Figure 7. Interplay between Arcuate Nucleus DII and UCP2 in Fuel Sensing

Under fed conditions (A), peripheral anorexigenic hormones, such as leptin, control the melanocortin system. During fasting (B), anorexigenic hormones, such as ghrelin, reverse the tone of the melanocortin system so that NPY/AgRP neuronal activity dominates. At the same time, elevating corticosteroid levels trigger DII activity and local T3 production, which trigger UCP2 production and activity in mitochondria (red) in NPY/AgRP neurons. The elevated activity of NPY/AgRP neurons suppresses POMC tone. We predict that by the time of refeeding (C), activated UCP2 has increased mitochondrial number in NPY/AgRP neurons, which, in turn, is a critical factor in sustaining an increased firing rate by these orexigenic cells so that food intake remains elevated and POMC neuronal firing stays suppressed subsequent to refeeding, at a time when neither circulating orexigenic nor anorexigenic signals dominate.

these animals exhibited a median frequency of spikes per minute significantly lower than that of wild-type animals. It is interesting to note, however, that NPY neurons in the arcuate nucleus showed a heterogeneity in their electrophysiological response to fasting suggesting that this neuronal population is more diverse in its functions than previously thought.

Strengthening our conclusions that an interplay between arcuate T3 and UCP2 in the hypothalamic regulation of energy balance exists, both DIIKO mice and *UCP2* KO animals had impaired elevation in *NPY* mRNA levels and rebound feeding following fasting.

The arcuate nucleus has emerged as a key region in the central regulation of energy metabolism housing the cell bodies of the melanocortin system, the NPY/AgRP neurons and the POMC-producing perikarya. Under satiety conditions, the adipose hormone leptin downregulates the activity of the NPY/AgRP neurons and promotes α-MSH neuronal activity (see Schwartz et al., 2000; Zigman and Elmquist, 2003; Horvath and Diano, 2004; Stanley et al., 2005 for review). During fasting, leptin levels rapidly decline while circulating corticosteroid and ghrelin levels rise, a process that is associated with increased NPY/AgRP and decreased α-MSH neuronal stimulation (Schwartz et al., 2000; Zigman and Elmquist, 2003). While ghrelin can directly alter the neuronal activity of the melanocortin system (Cowley et al., 2003), elevated corticosteroid levels will trigger glial DII activity (Coppola et al., 2005a) in hypothalamic tanycytes and astrocytes and, consequently, the local production of T3 (Coppola et al., 2005b). Our present results indicate that this increase in hypothalamic T3 production may have an indirect action on neuronal functions mediated by UCP2 and that this process plays a role in the physiological regulation of feeding.

In summary, we suggest that hypothalamic DII-derived T3 triggers activation of neuronal UCP2 that, in turn, elevates the activity level of NPY/AgRP neurons. Our results indicate that this mechanism is critical in sustaining an increased firing rate in these orexigenic cells so that appetite remains elevated during fasting (Figure 7). Overall, our study provides strong evidence for an interplay between local T3 production and UCP2 during fasting and reveals a central thermogenic-like mechanism (Horvath et al., 1999; Andrews et al., 2005b) in the regulation of food intake (Figure 7).

EXPERIMENTAL PROCEDURES

Double Immunocytochemistry for DII and GFP

Adult C57BL/6 mice carrying GFP in NPY/AgRP neurons (Pinto et al., 2004) were used in this study. Animals were perfused as previously described (Pinto et al., 2004).

For immunofluorescence microscopy, brain sections were immunostained with rabbit anti-DII (1:500) and subsequently with Alexa Fluor 594 donkey anti-rabbit IgG (Molecular Probes).

For electron microscopy, the immunolabeling for DII was carried as previously reported (Diano et al., 2003a). Sections were further incubated with a mouse anti-GFP antibody (Molecular Probes; 1:4000), and the immunoreactivity was visualized with DAB. Ribbons of ultrathin sections (Leica Ultramicrotome) were collected and examined using an FEI Biotwin electron microscope.

Combined GFP Immunostaining and In Situ Hybridization for UCP2

C57BL/6 mice carrying GFP in NPY/AgRP neurons were sacrificed by transaortic perfusion as previously reported (Richard et al., 1998).

Sections were first immunostained with a mouse anti-GFP antibody (Molecular Probes; 1:4000; immunoreactivity for GFP was visualized by DAB, resulting in a brown reaction product) and then processed for in situ hybridization for UCP2 as previously reported (Richard et al., 1998).

Determination of Hypothalamic and Serum T3 Levels

Ten male mice were sacrificed, and hypothalami were dissected, weighed, and stored at −80°C. Hypothalamic triiodothyronine (T3) was measured as previously described (Coppola et al., 2005b). T3 was expressed in pg/mg of wet tissue weight.

Serum free T3 levels were measured by RIA kit (Diagnostic Products Corporation) according to the manufacturer's protocol.

Brain Mitochondria Preparation and Uncoupling-Activity Measurements

Thirty-two male wild-type mice and thirty-two *UCP2* KO mice were used in this study and were divided into the following groups: 8 mice were single injected with T3 (5 μg), 8 were injected with saline, 8 were fasted for 24 hr, and 8 were fed ad libitum. Mice injected with saline or T3 were sacrificed 6 hr after injection. Animals were decapitated under deep anesthesia, and hypothalami were dissected. Mitochondria were isolated as previously reported (Andrews et al., 2005b). Protein concentrations were determined by a BCA protein assay kit (Pierce). Mitochondrial respirations were assessed using a Clark-type oxygen electrode (Hansatech Instruments) at 37°C as previously described (Andrews et al., 2005b). UCP-mediated proton conductance was measured as increased fatty-acid-induced respiration (Echtay et al., 2002), which was then compared with state 4 respiration induced by oligomycin, an inhibitor of H^+-transporting ATP synthase. All of the above determinations were performed in both the presence and absence of exogenous GDP (500 μM) in the respiration buffer.

Real-Time PCR for *UCP2* mRNA in Fasted, T3-Treated, and PTU+IOP-Treated Mice

Thirty male C57BL/6 mice were used in this study and were divided in the following groups: 5 mice were injected i.p. with T3 (5 μg), 5 controls were injected with saline, 5 were fasted for 24 hr, 5 were fed controls, 5 were hypothyroid, and 5 were euthyroid. Hypothyroidism was induced in mice by a daily i.p. injection of 6-*n*-propylthiouracil (PTU) (10 mg/kg body weight) together with iopanoic acid (IOP) (100 mg/kg body weight) for 14 days. Euthyroid controls received a daily injection of vehicle control for 14 days.

T3- and saline-treated animals were sacrificed 6 hr after injection; hypothalami were dissected and processed for RNA extraction. Total RNA was extracted using TRIzol reagent (Invitrogen) according to the manufacturer's instructions. Reverse transcription was performed by the First-Strand cDNA Synthesis Kit (Amersham Biosciences) using 3 μg of total RNA in 15 μl of total volume. Real-time PCR analysis of *UCP2* mRNA levels was performed by using iQ SYBR Green Supermix (Bio-Rad) and 0.5 μM of each primer (sense: 5′-CTACAAGACCA TTGCACGAGAGG-3′; antisense: 5′-AGCTGCTCATAGGTGACAAAC AT-3′). Primers against 18S RNA were included as controls. Measurements were performed on an iCycler (Bio-Rad).

Quantification of Mitochondria in GFP-NPY/AgRP Cells of the Arcuate Nucleus

For this experiment, we used adult C57BL/6 mice carrying GFP in NPY/AgRP neurons (Pinto et al., 2004) that were divided in two groups: 5 mice were fasted for 24 hr, and 5 mice were fed ad libitum. Animals were perfused as described above, and their brains were processed for GFP immunolabeling for electron microscopic examination. The unbiased stereological method for the assessment of mitochondrial number that was used was based on Pinto et al. (2004). The central feature of this approach is the use of a systematic random sampling method, which meets the statistical requirements necessary to ensure an unbiased estimate of the feature of interest. In selecting a sample series, the first section to be analyzed was randomly selected from an initial interval of sections, which then defined the spacing of the remaining sections to be examined. Thus, if we chose to sample every tenth section to measure mitochondrial number, the starting point of the series for each animal was randomly selected among the first ten sections, and then every tenth section was taken from this starting point through the remainder of the series. Having defined a series of sections with equal spacing of a known distance (t), it is then possible to estimate the volume of the structure of interest using the Cavalieri method (Gundersen and Jensen, 1987; Gundersen et al., 1988). Briefly, a point-counting grid with a defined area between points a(p), which is corrected for the magnification at which the section is viewed or drawn, was superimposed over the drawing or image of each section in the series. The number of grid points intersecting the structure of interest (*P) is then calculated for each section, and the volume (v) of the region of interest is calculated by the formula $v = *P \times a(p) \times t$. The assessment of mitochondrial number was determined using the optical dissector method on electron micrographs. Here, sections to be sampled were selected as above, and smaller grid areas were chosen from within each section in a similar systematic random manner. These areas (typically 100 μm^2) were then used to count mitochondria in GFP-immunopositive cells. Within each area, an optical section was established between the surfaces of the tissue section, thus creating a three-dimensional sampling area of known dimensions. All mitochondrial planes within this area were counted, provided that they did not cross three of the borders of the sampling boxes considered as exclusionary borders. The counts obtained from these sampling boxes were determined and represent the number of mitochondria per unit volume of the structure of interest. These counts were then corrected for the total volume of the structure obtained with the Cavalieri method, yielding a value for total mitochondrial number for the cell class and structure sampled.

In Situ Hybridization for c-Fos in *UCP2* KO Mice

In situ hybridization was performed on adult *UCP2* KO mice and their WT littermates (n = 4) fasted for 24 hr. Twenty-five μm thick sections were processed for c-Fos in situ hybridization as described by Timofeeva et al. (2005).

Double Immunostaining for c-Fos and GFP in Fasted *UCP2* KO and Wild-Type Mice

Five adult *UCP2* KO mice carrying GFP in NPY/AgRP neurons and five wild-type mice carrying GFP in NPY/AgRP neurons were housed singly and fasted for 24 hr. Animals were then perfused as described above.

Brain sections were incubated with rabbit anti-c-Fos (1:20,000 in PB-Triton X-100; Calbiochem) overnight at room temperature and then incubated in Alexa Fluor 594 donkey anti-rabbit IgG (1:200; Molecular Probes). The number of c-Fos-immunopositive nuclei as well as the number of cells double immunostained for c-Fos and GFP were counted using ScionImage (NIH).

Real-Time PCR for *NPY* mRNA in *UCP2* KO, WT Controls, and DIIKO and WT Control Mice

Forty male mice were used in this study and were divided into the following groups: 5 *UCP2* KO mice were fasted for 24 hr, 5 *UCP2* KO were fed controls, 5 WT were fasted for 24 hr, 5 WT were fed controls, 5 DIIKO were fasted for 24 hr, 5 DIIKO were fed controls, 5 WT were fasted for 24 hr, and 5 WT were fed controls. Mice were sacrificed and hypothalami were dissected. Total RNA extraction and reverse transcription were performed as described above. Real-time PCR analysis of *NPY*, *POMC*, and *ANT* mRNA levels was performed by using iQ SYBR Green Supermix (Bio-Rad) and 0.5 μM of each primer (NPY sense primer: 5′-GCTAGGTAACAACGAATGGGG-3′; NPY antisense primer: 5′-CACATGGAAGGGTCTTCAAGC-3′; POMC sense primer: 5′-GGCCTTTCCCCTAGAGTTCA-3′; POMC antisense primer: 5′-TTGATGATGGCGTTCTTGAA-3′; ANT sense primer: 5′-GGACAG ATTCTCTGGGCTTG-3′; ANT antisense primer 5′-TGGAAATGGCTT TAAGAGAAAAC-3′). Primers against 18S RNA were included as controls. Measurements were performed on an iCycler (Bio-Rad).

Quantification of Mitochondria in the Arcuate GFP-NPY/AgRP Neurons of *UCP2* KO and WT Controls after 24 hr Food Deprivation

Adult *UCP2* KO mice and WTs carrying GFP in NPY/AgRP neurons were used. Five *UCP2* KO and five WT mice were fasted for 24 hr. Animals were perfused as described above, and their brains were processed for GFP immunolabeling for electron microscopic examination as described above. The unbiased stereological method for the assessment of mitochondrial number was used as described above.

Firing Rate of Fasted NPY/AgRP Neurons in *UCP2* KO and Wild-Type Mice

GFP-NPY animals were sacrificed, and brains were rapidly removed, immersed in cold (4°C) oxygenated bath solution (containing [in mM] 220 sucrose, 2.5 KCl, 1 $CaCl_2$, 6 $MgCl_2$, 1.25 NaH_2PO_4, 26 $NaHCO_3$, 10 glucose [pH 7.3] with NaOH), and trimmed to a large block containing the hypothalamus. Coronal slices (180 μm) were cut through the full extent of the arcuate nucleus and maintained in a holding chamber with ASCF (bubbled with 5% CO_2 and 95% O_2) containing (in mM) 124 NaCl, 3 KCl, 2 $CaCl_2$, 2 $MgCl_2$, 1.23 NaH_2PO_4, 26 $NaHCO_3$, 2.5 glucose (pH 7.4) with NaOH. Slices were transferred to a recording chamber after at least 1 hr recovery and were constantly perfused with bath solution (33°C) at 2 ml/min. Slices were maintained for 1 hr at 35°C in 95% O_2/5% CO_2-saturated ACSF prior to recordings. We routinely obtained six usable slices containing GFP neurons from each mouse. A slice was then placed on the stage of an upright hybrid fluorescence/infrared microscope with long working distance objectives (Olympus BX51WI), and the presence of fluorescent cells was verified. Fluorescence filter sets appropriate for sapphire FP, cyan FP, and GFP (Chroma Technology Corp.) were used to confirm cell fluorescence. The slices were perfused with oxygenated ACSF at 35°C. Using established criteria, an appropriate healthy fluorescent cell was visually selected. Extracellular recordings were made with a glass electrode filled with ACSF (resistance = 2–5 MΩ) with a multiclamp 700A amplifier (Axon Instruments, Inc.) in the hypothalamic slices from mice. The recording electrode was propelled by a motorized micromanipulator to approach an identified GFP-NPY neuron. A loose seal was formed (resistance = 10–20 MΩ) when the micropipette touched the surface of a neuron. Ten minutes of spontaneous spikes was recorded from each neuron. Cumulative probability curves of frequency of spikes obtained from wild-type and *UCP2* KO mice were plotted using KaleidaGraph and examined with the Kolmogorov-Smirnov test using GB-STAT software.

Fasting and Refeeding in *UCP2* KO Mice

Five male *UCP2* KO and five wild-type mice were fasted for 24 hr. Food was replaced after 24 hr, at which time food intake was measured in a 60 min period following refeeding.

Fasting and Refeeding in DIIKO Mice

Fifteen male DIIKO and six wild-type mice (Schneider et al., 2001) were fasted for 24 hr. Six hours before food was replaced, 7 DIIKO mice were injected i.p. with T3 (5 μg/30 g body weight) and 8 DIIKO mice and the 6 wild-type mice were injected with saline. Food was replaced 24 hr after fasting, at which time food intake was measured in a 30 min period following refeeding.

ACKNOWLEDGMENTS

To Nicola Diano con l'amore di sempre. We thank P.R. Larsen and V.A. Galton for the DIIKO animals, E. Borok for superb technical assistance, and M. Shanabrough for editing the manuscript. This work was supported by NIH grants DK061619 and DK070039 to S.D.; DK070723 to X.-B.G.; and DK074386, DK060711, and AG022880 to T.L.H. and a grant from the Juvenile Diabetes Research Foundation to S.D.

Received: March 8, 2006
Revised: October 26, 2006
Accepted: December 7, 2006
Published: January 2, 2007

REFERENCES

Andrews, Z.B., Diano, S., and Horvath, T.L. (2005a). Mitochondrial uncoupling proteins in the CNS: in support of function and survival. Nat. Rev. Neurosci. *6*, 829–840.

Andrews, Z.B., Horvath, B., Barnstable, C.J., Elseworth, J., Yang, L., Beal, M.F., Roth, R.H., Matthews, R.T., and Horvath, T.L. (2005b). Uncoupling protein-2 is critical for nigral dopamine cell survival in a mouse model of Parkinson's disease. J. Neurosci. *25*, 184–191.

Andrews, Z.B., Rivera, A., Elsworth, J., Roth, R., Agnati, L., Gago, B., Abizaid, A., Schwartz, M., Fuxe, K., and Horvath, T.L. (2006). Uncoupling protein-2 promotes nigrostriatal dopamine neuronal function. Eur. J. Neurosci. *24*, 32–36.

Arsenijevic, D., Onuma, H., Pecqueur, C., Raimbault, S., Manning, B.S., Miroux, B., Couplan, E., Alves-Guerra, M.C., Goubern, M., Surwit, R., et al. (2000). Disruption of the uncoupling protein-2 gene in mice reveals a role in immunity and reactive oxygen species production. Nat. Genet. *26*, 435–439.

Bassett, J.H., Harvey, C.B., and Williams, G.R. (2003). Mechanisms of thyroid hormone receptor-specific nuclear and extra nuclear actions. Mol. Cell. Endocrinol. *213*, 1–11.

Brand, M.D., and Esteves, T.C. (2005). Physiological functions of the mitochondrial uncoupling proteins UCP2 and UCP3. Cell Metab. *2*, 85–93.

Brustovetsky, N., and Klingenberg, M. (1994). The reconstituted ADP/ATP carrier can mediate H+ transport by free fatty acids, which is further stimulated by mersalyl. J. Biol. Chem. *269*, 27329–27336.

Brustovetsky, N.N., Dedukhova, V.I., Egorova, M.V., Mokhova, E.N., and Skulachev, V.P. (1990). Inhibitors of the ATP/ADP antiporter suppress stimulation of mitochondrial respiration and H^+ permeability by palmitate and anionic detergents. FEBS Lett. *272*, 187–189.

Coppola, A., Meli, R., and Diano, S. (2005a). Inverse shift in circulating corticosterone and leptin levels elevates hypothalamic deiodinase type 2 in fasted rats. Endocrinology *146*, 2827–2833.

Coppola, A., Hughes, J., Esposito, E., Schiavo, L., Meli, R., and Diano, S. (2005b). Suppression of hypothalamic deiodinase type II activity blunts TRH mRNA decline during fasting. FEBS Lett. *579*, 4654–4658.

Cowley, M.A., Smith, R., Diano, S., Tschöp, M., Pronchuk, N., Grove, K.L., Strasburger, C.J., Bidlingmaier, M., Esterman, M., Heiman, M.L., et al. (2003). The distribution and mechanism of action of ghrelin in the CNS demonstrates a novel hypothalamic circuit regulating energy homeostasis. Neuron *37*, 649–661.

Diano, S., Naftolin, F., Goglia, F., and Horvath, T.L. (1998a). Fasting-induced increase in type II iodothyronine deiodinase activity and messenger ribonucleic acid levels is not reversed by thyroxine in the rat hypothalamus. Endocrinology *139*, 2879–2884.

Diano, S., Naftolin, F., Goglia, F., and Horvath, T.L. (1998b). Monosynaptic pathway between the arcuate nucleus expressing glial type II iodothyronine 5′-deiodinase mRNA and the median eminence-projective TRH cells of the rat paraventricular nucleus. J. Neuroendocrinol. *10*, 731–742.

Diano, S., Leonard, J., Meli, R., Esposito, E., and Schiavo, L. (2003a). Hypothalamic type II iodothyronine deiodinase: a light and electron microscopic study. Brain Res. *976*, 130–134.

Diano, S., Matthews, R.T., Patrylo, P., Yang, L., Beal, M.F., Barnstable, C.J., and Horvath, T.L. (2003b). Uncoupling protein 2 prevents neuronal death including that occurring during seizures: a mechanism for preconditioning. Endocrinology *144*, 5014–5021.

Dummler, K., Muller, S., and Seitz, H.J. (1996). Regulation of adenine nucleotide translocase and glycerol 3-phosphate dehydrogenase expression by thyroid hormones in different rat tissues. Biochem. J. *317*, 913–918.

Echtay, K.S., Roussel, D., St-Pierre, J., Jekabsons, M.B., Cadenas, S., Stuart, J.A., Harper, J.A., Roebuck, S.J., Morrison, A., Pickering, S.,

et al. (2002). Superoxide activates mitochondrial uncoupling proteins. Nature *415*, 96–99.

Gropp, E., Shanabrough, M., Borok, E., Xu, A.W., Janoschek, R., Buch, T., Plum, L., Balthasar, N., Hampel, B., Waisman, A., et al. (2005). Agouti-related peptide-expressing neurons are mandatory for feeding. Nat. Neurosci. *8*, 1289–1291.

Gundersen, H.J., and Jensen, E.B. (1987). The efficiency of systematic sampling in stereology and its prediction. J. Microsc. *147*, 229–263.

Gundersen, H.J., Bendtsen, T.F., Korbo, L., Marcussen, N., Moller, A., Nielsen, K., Nyengaard, J.R., Pakkenberg, B., Sorensen, F.B., Vesterby, A., et al. (1988). Some new, simple and efficient stereological methods and their use in pathological research and diagnosis. APMIS *96*, 379–394.

Harvey, C.B., and Williams, G.R. (2002). Mechanism of thyroid hormone action. Thyroid *12*, 441–446.

Horrum, M.A., Tobin, R.B., and Ecklund, R.E. (1990). Thyroid hormone effects on the proton permeability of rat liver mitochondria. Mol. Cell. Endocrinol. *68*, 137–141.

Horvath, B., Spies, C., Warden, C., Diano, S., and Horvath, T.L. (2002a). Uncoupling protein 2 in primary pain and temperature afferents of the spinal cord. Brain Res. *955*, 260–263.

Horvath, B., Spies, C., Horvath, G., Kox, W.J., Miyamoto, S., Barry, S., Warden, C.H., Bechmann, I., Diano, S., Heemskerk, J., and Horvath, T.L. (2002b). Uncoupling protein 2 (UCP2) lowers alcohol sensitivity and pain threshold. Biochem. Pharmacol. *64*, 369–374.

Horvath, T.L., Warden, C.H., Hajos, M., Lombardi, A., Goglia, F., and Diano, S. (1999). Brain UCP2: uncoupler neuronal mitochondria predict thermal synapses in homeostatic centers. J. Neurosci. *19*, 10417–10427.

Horvath, T.L., Diano, S., Miyamoto, S., Barry, S., Gatti, S., Alberati, D., Livak, F., Lombardi, A., Moreno, M., Goglia, F., et al. (2003). Uncoupling proteins-2 and 3 influence obesity and inflammation in transgenic mice. Int. J. Obes. *27*, 433–442.

Horvath, T.L., and Diano, S. (2004). The floating blueprint of hypothalamic feeding circuits. Nat. Rev. Neurosci. *5*, 662–667.

Kalderon, B., Hermesh, O., and Bar-Tana, J. (1995). Mitochondrial permeability transition is induced by in vivo thyroid hormone treatment. Endocrinology *136*, 3552–3556.

Klingenspor, M. (2003). Cold-induced recruitment of brown adipose tissue thermogenesis. Exp. Physiol. *88*, 141–148.

Krauss, S., Zhang, C.Y., and Lowell, B.B. (2005). The mitochondrial uncoupling-protein homologues. Nat. Rev. Mol. Cell Biol. *6*, 248–261.

Lanni, A., De Felice, M., Lombardi, A., Moreno, M., Fleury, C., Ricquier, D., and Goglia, F. (1997). Induction of UCP2 mRNA by thyroid hormones in rat heart. FEBS Lett. *418*, 171–174.

Lanni, A., Moreno, M., Lombardi, A., and Goglia, F. (2003). Thyroid hormone and uncoupling proteins. FEBS Lett. *543*, 5–10.

Lechan, R.M., Qi, Y.P., Berrodin, T.J., Davis, K.D., Schwartz, H.L., Strait, K.A., Oppenheimer, J.H., and Lazar, M.A. (1993). Immunocytochemical delineation of thyroid hormone receptor beta 2-like immunoreactivity in the rat central nervous system. Endocrinology *132*, 2461–2469.

Li, Z., Okamoto, K., Hayashi, Y., and Sheng, M. (2004). The importance of dendritic mitochondria in the morphogenesis and plasticity of spines and synapses. Cell *119*, 873–887.

Luquet, S., Perez, F.A., Hnasko, T.S., and Palmiter, R.D. (2005). NPY/AgRP neurons are essential for feeding in adult mice but can be ablated in neonates. Science *310*, 683–685.

Masaki, T., Yoshimatsu, H., Kakuma, T., Hidaka, S., Kurokawa, M., and Sakata, T. (1997). Enhanced expression of uncoupling protein 2 gene in rat white adipose tissue and skeletal muscle following chronic treatment with thyroid hormone. FEBS Lett. *418*, 323–326.

Nedergaard, J., Ricquier, D., and Kozak, L.P. (2005). Uncoupling proteins: current status and therapeutic prospects. EMBO Rep. *6*, 917–921.

Pinto, S., Roseberry, A.G., Liu, H., Diano, S., Shanabrough, M., Cai, X., Friedman, J.M., and Horvath, T.L. (2004). Rapid rewiring of arcuate nucleus feeding circuits by leptin. Science *304*, 110–115.

Reitman, M.L., He, Y., and Gong, D.W. (1999). Thyroid hormone and other regulators of uncoupling proteins. Int. J. Obes. Relat. Metab. Disord. *23* (*Suppl 6*), S56–S59.

Richard, D., Rivest, R., Huang, Q., Bouillaud, F., Sanchis, D., Champigny, O., and Ricquier, D. (1998). Distribution of the uncoupling protein 2 mRNA in the mouse brain. J. Comp. Neurol. *397*, 549–560.

Ricquier, D. (2005). Respiration uncoupling and metabolism in the control of energy expenditure. Proc. Nutr. Soc. *64*, 47–52.

Rowland, K.C., Irby, N.K., and Spirou, G.A. (2000). Specialized synapse-associated structures within the calyx of Held. J. Neurosci. *20*, 9135–9144.

Schneider, M.J., Fiering, S.N., Pallud, S.E., Parlow, A.F., St Germain, D.L., and Galton, V.A. (2001). Targeted disruption of the type 2 selenodeiodinase gene (DIO2) results in a phenotype of pituitary resistance to T4. Mol. Endocrinol. *15*, 2137–2148.

Schuman, E., and Chan, D. (2004). Fueling synapses. Cell *119*, 738–740.

Schwartz, M.W., Woods, S.C., Porte, D., Jr., Seeley, R.J., and Baskin, D.G. (2000). Central nervous system control of food intake. Nature *404*, 661–671.

Sell, H., Deshaies, Y., and Richard, D. (2004). The brown adipocyte: update on its metabolic role. Int. J. Biochem. Cell Biol. *36*, 2098–2104.

Shepherd, G.M., and Harris, K.M. (1998). Three-dimensional structure and composition of CA3→CA1 axons in rat hippocampal slices: implications for presynaptic connectivity and compartmentalization. J. Neurosci. *18*, 8300–8310.

Silva, J.E. (1995). Thyroid hormone control of thermogenesis and energy balance. Thyroid *5*, 481–492.

Skulachev, V.P. (1991). Fatty acid circuit as a physiological mechanism of uncoupling of oxidative phosphorylation. FEBS Lett. *294*, 158–162.

Skulachev, V.P. (1998). Uncoupling: new approaches to an old problem of bioenergetics. Biochim. Biophys. Acta *1363*, 100–124.

Stanley, S., Wynne, K., McGowan, B., and Bloom, S. (2005). Hormonal regulation of food intake. Physiol. Rev. *85*, 1131–1158.

Takahashi, K.A., and Cone, R.D. (2005). Fasting induces a large, leptin-dependent increase in the intrinsic action potential frequency of orexigenic arcuate nucleus neuropeptide Y/Agouti-related protein neurons. Endocrinology *146*, 1043–1047.

Timofeeva, E., Baraboi, E.D., and Richard, D. (2005). Contribution of the vagus nerve and lamina terminalis to brain activation induced by refeeding. Eur. J. Neurosci. *22*, 1489–1501.

Tu, H.M., Kim, S., Salvatore, D., Bartha, T., Legradi, G., Larsen, P.R., and Lechan, R.M. (1997). Regional distribution of type 2 thyroxine deiodinase messenger ribonucleic acid in rat hypothalamus and pituitary and its regulation by thyroid hormone. Endocrinology *138*, 3359–3368.

Weitzel, J.M., Iwen, K.A., and Seitz, H.J. (2003). Regulation of mitochondrial biogenesis by thyroid hormone. Exp. Physiol. *88*, 121–128.

Zhang, C.Y., Baffy, G., Perret, P., Krauss, S., Peroni, O., Grujic, D., Hagen, T., Vidal-Puig, A.J., Boss, O., Kim, Y.B., et al. (2001). Uncoupling protein-2 negatively regulates insulin secretion and is a major link between obesity, beta cell dysfunction, and type 2 diabetes. Cell *105*, 745–755.

Zigman, J.M., and Elmquist, J.K. (2003). Minireview: From anorexia to obesity—the yin and yang of body weight control. Endocrinology *144*, 3749–3756.